



OPEN

DATA DESCRIPTOR

A curated binary pattern multitarget dataset of focused ATP-binding cassette transporter inhibitors

Sven Marcel Stefan ^{1,2,3,4}, Patric Jan Jansson ^{3,5}, Jens Pahnke ^{1,4,6,7} & Vigneshwaran Namasivayam ^{2,4} ✉

Multitarget datasets that correlate bioactivity landscapes of small-molecules toward different related or unrelated pharmacological targets are crucial for novel drug design and discovery. ATP-binding cassette (ABC) transporters are critical membrane-bound transport proteins that impact drug and metabolite distribution in human disease as well as disease diagnosis and therapy. Molecular-structural patterns are of the highest importance for the drug discovery process as demonstrated by the novel drug discovery tool 'computer-aided pattern analysis' ('C@PA'). Here, we report a multitarget dataset of 1,167 ABC transporter inhibitors analyzed for 604 molecular substructures in a statistical binary pattern distribution scheme. This binary pattern multitarget dataset (ABC_BPMDs) can be utilized for various areas. These areas include the intended design of (i) polypharmacological agents, (ii) highly potent and selective ABC transporter-targeting agents, but also (iii) agents that avoid clearance by the focused ABC transporters [e.g., at the blood-brain barrier (BBB)]. The information provided will not only facilitate novel drug prediction and discovery of ABC transporter-targeting agents, but also drug design in general in terms of pharmacokinetics and pharmacodynamics.

Background & Summary

The superfamily of ABC transporters is of highest importance in terms of novel drug discovery, design, and development. ABC transporters are ubiquitously present in the human body^{1–4}, and their (co-)expression has broad implications in human diseases. These diseases include prevalent [e.g., Alzheimer's disease (AD)^{5,6}, atherosclerosis⁷, or cancer^{1,3,6,8}] and orphan [e.g., Tangier disease (ABCA1)⁹, Stargardt's disease (ABCA4)¹⁰, harlequin ichthyosis (ABCA12)¹¹, pseudoxanthoma elasticum (ABCC6)¹², or adrenoleukodystrophy (ABCD1)¹³] pathological conditions. Together with tight-junction proteins, these membrane-bound efflux pumps are the backbone of systemic barrier formation^{14,15}. Their localization at blood-tissue barriers impacts metabolite distribution and drug delivery, and hence, disease progress, treatment, and therapy^{15–19}. Determinants that establish a correlation between the molecular structure of a small-molecule (drug) and its interaction with ABC transporters is key for the development of novel, safe, systemically applicable, and target-oriented (selective) drugs.

These determinants include descriptors that conserve certain physicochemical features of the small-molecules of interest, such as the calculated octanol-water partition coefficient (CLogP), molecular weight

¹Department of Pathology, Section of Neuropathology, Translational Neurodegeneration Research and Neuropathology Lab (www.pahnkelab.eu), University of Oslo and Oslo University Hospital, Sognsvannsveien 20, 0372 Oslo, Norway. ²Department of Pharmaceutical and Cellbiological Chemistry, Pharmaceutical Institute, University of Bonn, An der Immenburg 4, 53121 Bonn, Germany. ³Cancer Drug Resistance & Stem Cell Program, School of Medical Science, Faculty of Medicine and Health, The University of Sydney, Camperdown, NSW 2006, Australia. ⁴LIED, Pahnke Lab, University of Lübeck and University Medical Center Schleswig-Holstein, Ratzeburger Allee 160, 23538 Lübeck, Germany. ⁵Bill Walsh Translational Cancer Research Laboratory, Kolling Institute, Faculty of Medicine and Health, The University of Sydney, St. Leonards, NSW 2065, Australia. ⁶Department of Pharmacology, Faculty of Medicine, University of Latvia, Jelgavas iela 4, 1004 Riga, Latvia. ⁷Department of Neurobiology, The Georg S. Wise Faculty of Life Sciences, Tel Aviv University, P.O. Box 39040, 6997801, Tel Aviv, Israel. ✉e-mail: vnamasiv@uni-bonn.de

(MW), molar refractivity (MR), or topological polar surface area (TPSA), but also the number of hydrogen bond (H-bond) donors, H-bond acceptors, or rotatable bonds⁵. Other than that, more complex attributes can be summarized in fingerprints that represent certain molecular features of the small-molecule in a binary code (e.g., feature-, path-, and radial-fingerprints^{20–22}). Unfortunately, comprehensive binary datasets do not exist for ABC transporters. However, the knowledge about such binary fingerprints could facilitate the development of (i) drugs that avoid clearance mediated by ABC transporters [e.g., targeting the BBB to treat central nervous system-(CNS)-related diseases²³]; (ii) agents targeting ABC transporters to study their expression and/or function with state-of-the-art imaging techniques [e.g., by positron emission tomography (PET)¹⁶]; (iii) drugs that selectively target well-studied ABC transporters in human diseases (e.g., cancer^{1,3,4,6,8}); (iv) broad-spectrum drugs that target several ABC transporters to ameliorate/cure an ABC transporter-associated pathological condition²⁴; (v) polypharmacological agents to target and study particularly less- and under-studied ABC transporters by a multitargeting approach^{7,25–27}; or (vi) combined/extended fingerprints to create high-quality compound collections that would provide a starting point of polypharmacology-focused virtual screenings⁷.

In the present work, we combined the concepts of the multitarget dataset^{7,27} and the binary distribution of substructures⁷. The latest version of the multitarget dataset contains 1,167 compounds that were evaluated against the well-studied ABC transporters ABCB1, ABCC1, and ABCG2. A large substructure catalog was created, containing in total 604 active (= present) substructures within these 1,167 compounds of the updated multitarget dataset. The new binary pattern multitarget dataset (ABC_BPMDS) is freely available under the <http://www.zenodo.org>²⁸ URL as well as the <http://www.panabc.info> website, and its use is free of charge.

Methods

The generation of the ABC_BPMDS was a four-step process: (i) deep literature search including the selection of qualified reports, resulting in the exquisite compilation of the original multitarget dataset as reported earlier²⁷ [including updates in our former⁷ and the present work (see below)]; (ii) manual curation of the given data, in particular: (a) calculation of bioactivity values for estimated bioactivity data and data determination, (b) unification and harmonization of bioactivity data, as well as (c) comparison, curation, and harmonization of molecular-structural data (SMILES codes); (iii) generation of a substructure catalog, in particular: (a) visual inspection of the 1,167 molecules of the updated multitarget dataset, (b) extraction of partial structures, (c) creation and extension of substitution patterns, as well as (d) screening of the multitarget dataset for these substructures, discovering 604 active substructures; and (iv) individual pattern analysis⁷ for uncovering the statistical distribution of these 604 active substructures amongst the 1,167 compounds of the multitarget dataset. The following sections will provide a detailed description on how the final ABC_BPMDS was assembled. Figure 1 provides an overview of the taken steps.

Literature Collection of the Original Dataset. *Qualified Reports.* A deep literature search was the first step to compile the original multitarget dataset, which has been reported in detail before^{7,27}. The National Center for Biotechnological Information (NCBI; <https://www.ncbi.nlm.nih.gov>)²⁹ was used to search for qualified reports applying the keywords (i) 'ABCB1', (ii) 'ABCC1', (iii) 'ABCG2', (iv) 'P-gp', (v) 'MRP1', and (vi) 'BCRP'. The keywords were used in all possible combinations to extract the maximal yield in reports. In addition to the genuine database search, the reference sections of the found reports were searched for potential additional literature to extract further qualified information.

Compounds. Compounds were considered only if they had been evaluated against all three focused targets, ABCB1, ABCC1, and ABCG2, including inactive compounds as well as selective, dual, and triple inhibitors. This information could be provided either in one single report (e.g., in case of the standard ABCG2 inhibitor Ko143³⁰) or in several individual reports [e.g., in case of the standard ABCC1 inhibitor verlukast (MK571)^{31–36}]. The molecular structures of qualified compounds were collected as SMILES codes. These were obtained either from (i) supplementary information of the respective report; (ii) the PubChem database (<https://pubchem.ncbi.nlm.nih.gov>)³⁷ [e.g., in case of known drugs and drug-like compounds, such as the standard inhibitors verapamil (ABCB1), cyclosporine A (ABCB1 and ABCC1), verlukast (ABCC1), or Ko143 (ABCG2)]; or (iii) manual drawing according to the 2D representations as outlined in the respective report using ChemDraw Pro version 20.1.1.125. Isomeric SMILES were considered where applicable. SMILES codes that encoded aromatic substructures with lower-case letters in certain reports^{38,39} were unified according to the upper-case description scheme (structural curation)⁷.

Assays. Only functional assays were considered using either fluorescence labeling or radionuclide detection applying either living (selected or transfected) cells or membrane vesicles with reconstituted transporters. ATPase assays were not considered because ATPase activity and transporter inhibition may not be directly connected to each other. MDR reversal assay data was not considered because of the complexity of the involved processes and the fact that the triggered response(s) may not only be caused by ABC transporter inhibition. Table 1 provides an exhaustive list of functional tracers (and substrates) that were used to assess the 1,167 compounds of the ABC_BPMDS against ABCB1, ABCC1, and ABCG2. Table 2 summarizes all used host systems (cell lines and membrane vesicles) used for the evaluation of the 1,167 compounds against ABCB1, ABCC1, and ABCG2.

Bioactivity. The bioactivities (IC₅₀ values) of the compounds were extracted from either (i) tables of the respective reports (including supplementary information); or (ii) screening figures with relative inhibition (I_{rel}) values (%) compared to a standard (I_{max}; 100%). In the latter case, the IC₅₀ values were estimated (either span or >, ≥, <, ~) in the previous multitarget dataset^{7,27}.

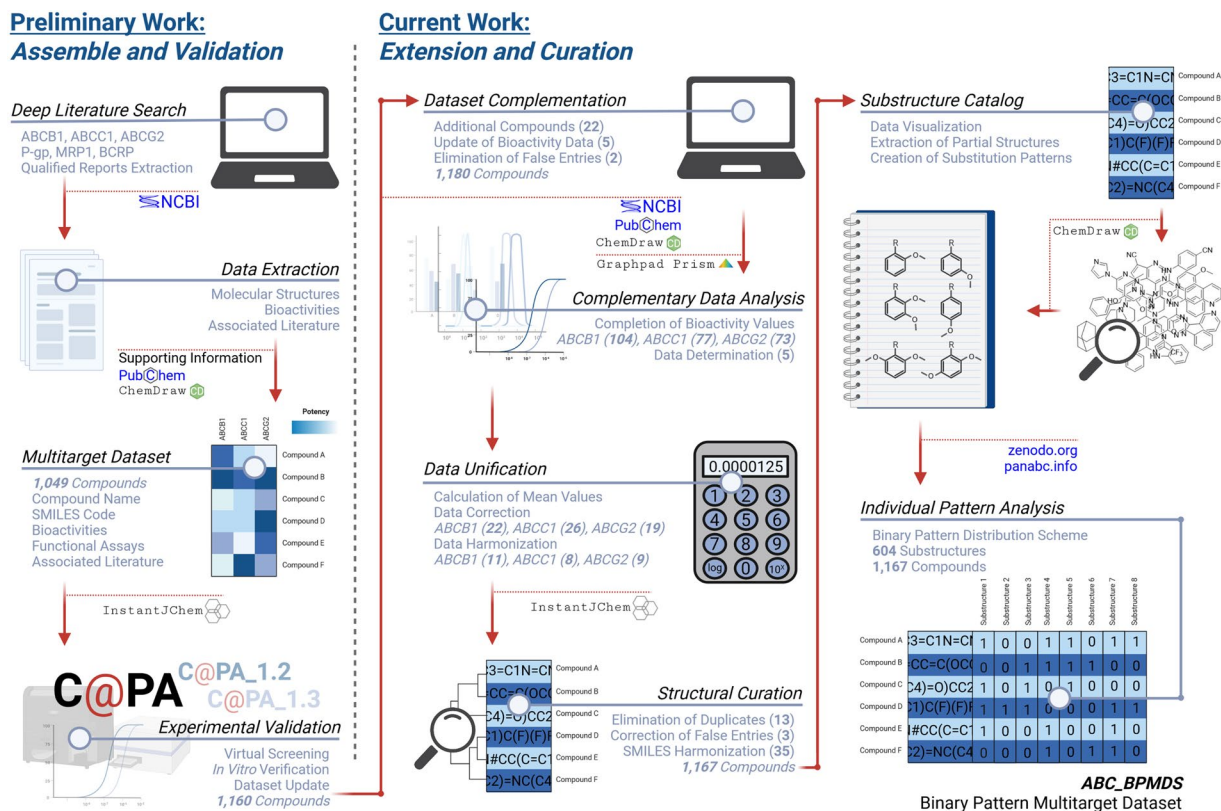


Fig. 1 Depiction of the main workflow of assemble and validation as reported earlier in our preliminary work²⁷, as well as the main steps of data extension and curation as part of the current work to generate the ABC_BPMDs. This graphic was created with BioRender.com (<https://biorender.com>).

Data Curation – Bioactivity Data. Dataset Update and Complementation. New reports particularly from 2021 and 2022 were taken into consideration to update the dataset with compounds that were evaluated against the three transporters ABCB1, ABCC1, and ABCG2. In total, 22 new compounds were included into the list of qualified compounds^{7,40–42}. In addition, we focused an extended literature search, particularly of known standard inhibitors of ABCB1, ABCC1, and ABCG2 to obtain bioactivities with less mathematical uncertainty which also align well with our empirical experience in the laboratory. These compounds included verapamil (ABCB1⁴³), cyclosporine A (ABCB1^{41,43–46} and ABCC1^{31,44–46}), verlukast (ABCC1^{31–36}), and Ko143 (ABCG2^{41,45}). As a side note, the additional literature search also resulted in an update of bioactivity data of the natural compound piperine⁴⁷. In the curation process to complement bioactivity values, we found that two compounds were erroneously included into the dataset (apatinib⁴⁸ and certinib⁴⁹). Both were not evaluated against ABCC1, and therefore, did not qualify for this dataset and were therefore removed.

Complementary Data Analysis. The bioactivity of several inhibitors could only be described as an estimation (either described as span, marked as ‘active’, or annotated with ‘>’, ‘≥’, ‘<’, ‘~’ in the previous dataset^{7,27}). However, to allow for the use of the entire dataset in mathematical and computational operations, we sought to allocate defined bioactivity values [e.g., screening figures, flow-cytometry histograms, or tables with bioactivity values other than IC₅₀ values (e.g., percentages)] were taken into consideration for further data analysis. The specific bioactivity value (e.g., percentage inhibition) was extracted and correlated to the used compound concentration. By using GraphPad Prism version 8.4.0 applying the three-parameter logistic equation with a fixed Hill slope (=1.0), IC₅₀ values were calculated and listed in the new multitarget dataset. A detailed curation protocol is provided on <https://www.zenodo.org>⁵⁰ as well as the <http://www.panabc.info> website, and the related GraphPad Prism file containing the concentration-effect curves can be accessed without restrictions. In total, the bioactivity data of 104, 77, and 73 ABCB1, ABCC1, and ABCG2 inhibitors, respectively, have been calculated and complemented.

Data Determination. The bioactivities of five compounds [ayanin⁵¹, retusin⁵¹ (flavone derivative 12⁵²), dihydrodibenzoazepine derivative 4i⁵³, dregamine derivative 2⁵⁴, and tabernaemontanine derivative 22⁵⁴] had to be determined without mathematical operations. The IC₅₀ values of ayanin and retusin were stated as ‘>50 μM’ in the original report⁵¹. Usually, these kinds of statements (e.g., ‘>50 μM’, ‘>100’, ‘inactive’, etc) led to the allocation of such compounds into the ‘inactive’ category (arbitrary IC₅₀ value of 2000 μM in the ABC_BPMDs). However, the authors of the respective publication stated that ayanin and retusin had some (weak) inhibitory activity⁵¹.

functional tracer	ABCB1 (P-gp)	ABCC1 (MRP1)	ABCG2 (BCRP)
BODIPY-FL-vinblastine ⁸⁴			
BODIPY-prazosin ⁸⁵			
Calcein AM ^{7,86}			
5-CFDA ⁸⁷			
DiOC _{2/3} ^{7,88}			
Daunorubicin ⁷			
Lucifer yellow ⁸⁹			
D-luciferin ⁹⁰			
Doxorubicin ⁹¹			
Estradiol glucuronide ⁹²			
Estrone sulfate ⁹³			
Fluo-3 AM ⁹⁴			
Fluo-4 AM ⁵⁵			
Hoechst 33342 ^{7,27}			
JC1 ⁹⁵			
Mitoxantrone ^{91,96,97}			
Paclitaxel ⁹⁸			
Rhodamine 123 ^{88,99,100}			
PhenGreen SK diacetate ⁸⁹			
Pheophorbide A ⁷			
N-methyl-quinidine ⁸⁹			
Rosuvastatin ¹⁰¹			
Silybin A ⁴⁷			
Silybin B ⁴⁷			
^{99m} Tc-Sestamibi ⁸⁷			
Vincristine ⁹⁴			

Table 1. An exhaustive list of functional tracers that were used to functionally assess the 1,167 compounds of the ABC_BPMDS against ABCB1, ABCC1, and ABCG2^{7,27}. The assessment of the corresponding transporter by the respective tracer is indicated by a black box. The provided references are examples in which details in terms of the stated assays can be found^{7,27,47,55,84–101}.

Therefore, we decided to allocate an arbitrary value of 100 μM to these compounds to acknowledge their minor inhibitory potential against ABCC1. Dihydrodibenzoazepine derivative 4i⁵³, dregamine derivative 25⁴, and tabernaemontanine derivative 22⁵⁴, on the other hand, reached over 100% inhibition at concentrations of 2.50 μM , 20.0 μM , and 20.0 μM , respectively. Unfortunately, these were the only indications of bioactivity by the authors of the original reports^{53,54}. Hence, we decided to allocate arbitrary values of 0.999 μM ⁵³, 4.99 μM ⁵⁴, and 4.99 μM ⁵⁴, respectively, to acknowledge their potentially (very) high inhibitory power against ABCB1 as well as ABCG2 considering the effect-concentrations used in the original reports. These arbitrary IC₅₀ values have been chosen since sub-classifications of bioactivity classes according to bioactivity thresholds (e.g., 1 and 5 μM) provided a better prediction in our previous works⁷.

Data Unification. Several compounds were evaluated in multiple assays, e.g., the mentioned standard inhibitors of ABCB1, ABCC1, and ABCG2. However, to allocate one bioactivity value to one compound, a unification process was necessary. As IC₅₀ values do not follow a normal distribution, the multiple IC₅₀ values associated with one compound were subject to a three-step mathematical operation: (i) logarithmization of the IC₅₀ values; (ii) calculation of the mean; and (iii) delogarithmization of the log(IC₅₀)-mean value. The resultant mean value was allocated to the respective compound. It shall be noted that the bioactivities of the compounds curcumin I-III (ABCC1)⁵⁵ and gefitinib (ABCB1 and ABCC1)⁵⁶ were only given as a span in the original reports^{55,56}, and hence, the mean of the respective span was taken for further operations. In total, 60, 48, and 209 ABCB1, ABCC1, and ABCG2 inhibitors have been given a new bioactivity value by these operations compared to the previous multitarget dataset^{7,27}.

Data Correction and Harmonization. Through the complementary analysis process, several bioactivity values were corrected. This applied for compounds that were falsely marked as ‘inactive’ in the previous multitarget dataset (ABCB1: 22 compounds; ABCC1: 26 compounds; ABCG2: 19 compounds)^{7,27}. Lastly, all bioactivity values of the ABC_BPMDS were harmonized according to a number of three significant digits. This harmonization resulted in a standardized format of presentation: (i) ‘XXX μM ’; (ii) ‘XXX μM ’; (iii) ‘XX.X μM ’; (iv) ‘X.XX μM ’; (v) ‘0.XXX μM ’; and (vi) ‘0.0XX (X = any numeric value between 1–9)’. Here, 11, 8, and 9 ABCB1, ABCC1, and ABCG2 values have been changed compared to the previous multitarget dataset^{7,27}.

cell line	ABCB1 (P-gp)	ABCC1 (MRP1)	ABCG2 (BCRP)
2008 ⁵²		<i>transfected</i>	
8226 ^{97,102}	doxorubicin (Dox6)		mitoxantrone (MR20)
A2780 ⁷	doxorubicin (ADR)		
A-459 ¹⁰³		cisplatin (DDP)	
BHK-21 ⁹⁹		<i>transfected</i>	
Caco-2 ¹⁰⁴			
CCRF ¹⁰⁵	doxorubicin (ADR5000)		
CORL-23 ⁸⁹		doxorubicin (R)	
Flp-In TM -293 ¹⁰⁶	<i>transfected</i>	<i>transfected</i>	<i>transfected</i>
H460 ¹⁰⁷			mitoxantrone (MX2)
H69 ⁷		doxorubicin (AR)	
HCT-15 ¹⁰⁸			
HEK293 ^{84,85,93}	<i>transfected vesicles</i>	<i>transfected vesicles</i>	<i>transfected vesicles</i>
HL60 ⁹⁷	vincristine (VCR)	doxorubicin (ADR)	
Ig ¹⁰⁵			mitoxantrone (MXP3)
Jurkat ¹⁰⁵	doxorubicin (DNR)		
K562 ^{42,102,109}	doxorubicin (A02) <i>transfected</i>	<i>transfected</i>	<i>transfected</i>
KB ^{48,84,107,110}	vinblastine (V1; V200; 8-5-11)	doxorubicin (C-A120)	
LLC-PK1 ¹⁰¹			<i>transfected</i>
MCF-7 ^{38,48,102,103,107,111}	doxorubicin (DOX)	doxorubicin (DOX) etoposide (VP16)	doxorubicin (DOX) flavopiridol (FLV1000) mitoxantrone (MX) topotecan (Topo) verapamil (AdrVp)
MDA-MB-231 ¹⁰⁰			<i>transfected</i>
MDCK ^{38,112}	<i>transfected vesicles</i>	<i>transfected</i>	<i>transfected</i>
MEF ¹¹³			<i>transduced</i>
MES-SA ¹¹⁴	doxorubicin (Dx-5)		mitoxantrone (MX2)
NIH-3T3 ⁹⁹	<i>transfected</i>		
PLB-985 ⁸⁹	<i>transfected</i>		<i>transfected</i>
S1 ⁴⁸			mitoxantrone (M1-80)
S9 ⁸⁹		<i>transfected, vesicles</i>	
SupT1 ¹⁰⁵		vincristine (Vin)	
SW620 ⁹⁸	doxorubicin (AD300)		

Table 2. An exhaustive list of transporter host systems that were used to functionally assess the 1,167 compounds of the ABC_BPMDS against the well-studied ABC transporters ABCB1, ABCC1, and ABCG2^{7,27}. The assessment of the corresponding transporter by the respective host system is indicated by a black box. Regarding selected cells, the used cytotoxic agent is indicated under the respective transporter, and the cell subline abbreviation is given in brackets. The provided references are examples in which details in terms of the stated cell lines can be found^{7,38,42,48,52,84,89,93,95,97-114}.

Data Curation – Molecular-structural Data. The 1,167 compounds of the ABC_BPMDS were portrayed as canonical or isomeric SMILES codes as derived from the (i) respective report, (ii) PubChem database (<https://pubchem.ncbi.nlm.nih.gov>), or (iii) SMILES generation tool of ChemDraw Pro version 20.1.1.125. All smiles were compared to each other to identify duplicates by using InstantJChem version 21.13.0. Through this individual cross-check of the molecular-structural data, 13 compounds were discovered as duplicates^{46,51,56-59} and their bioactivity values were merged with the original bioactivity data of the particular compound^{52,59-62}. In addition, three compounds were identified to be incorrect in terms of their molecular structure and have been corrected in the dataset^{46,57,63}.

Binary Pattern Generation. *Background.* In contrast to common molecular fingerprints for similarity-based virtual screenings^{20,64}, the very recently reported novel drug discovery tool ‘computer-aided pattern analysis’ (‘C@PA’) identified that defined (=non-substituted) hydrogens and their positioning is particularly important in terms of the differentiation between selective and multitarget inhibition of ABC transporters^{7,26,27}. Although certain fingerprints indeed consider polar hydrogens^{21,22}, C@PA particularly discovered non-polar

inhibitor class	count	IC ₅₀ span [μM]	pIC ₅₀ span	IC ₅₀ median [μM]	pIC ₅₀ median	IC ₅₀ mean [μM]	pIC ₅₀ mean
ABC_BPMDS	1,167	0.0153–1630	7.815–2.788	4.39	5.358	3.84	5.416
All ABCB1	525	0.0153–1460	7.815–2.836	6.37	5.196	6.32	5.199
All ABCC1	344	0.146–1630	6.836–2.788	11.2	4.951	9.26	5.033
All ABCG2	866	0.0234–405	7.631–3.393	1.95	5.710	2.00	5.698
Selective ABCB1	88	0.0153–708	7.815–3.150	2.51	5.599	3.41	5.467
Selective ABCC1	61	0.222–112	6.654–3.951	5.97	5.224	5.63	5.249
Selective ABCG2	409	0.0234–405	7.631–3.393	1.06	5.975	1.13	5.948
Dual ABCB1/ABCC1	38	0.289–180	6.539–3.745	20.4	4.692	15.2	4.819
Dual ABCC1/ABCG2	212	0.0255–333	7.593–3.478	4.43	5.354	3.85	5.415
Dual ABCC1/ABCG2	58	0.0988–163	7.005–3.788	10.1	4.996	6.92	5.160
Triple ABCB1/ABCC1/ABCG2	187	0.0475–1630	7.323–2.788	6.98	5.156	6.74	5.172

Table 3. Statistical survey of the span as well as median and mean values of the bioactivity of the entire ABC_{BPMDS} as well as important sub-classes. The pIC₅₀ values have been calculated by using the negative decadic logarithm of the respective bioactivity value.

hydrogens with critical discriminatory potential in the virtual screening process^{7,26,27}. However, the original C@PA worked with a very preliminary and limited dataset of 308 substructures which were compiled after multitarget dataset visualization and literature consideration⁶⁵, of which only 162 substructures were active in the multitarget dataset of, at the time of the study, 1,049 compounds²⁷.

Substructure Visualization, Identification, and Extension. For the development of a complete, detailed, and novel (multitarget) fingerprint, which may also universally be used in (multitarget) virtual screening approaches, the 1,167 compounds of the updated multitarget dataset were visualized using ChemDraw Pro version 20.1.1.125, and substructures were identified and extracted. The extracted substructures [e.g., single-standing/centered (hetero-)aromatic rings, condensed (hetero-)aromatic rings, (un)saturated side chains, extremities, and non-aromatic (hetero-)cycles, etc.] were derivatized by applying a heavy atom substitution scheme as already reported earlier²⁶ (scaffold fragmentation and substructure hopping). Especially the presence and positioning of (non-polar) hydrogens in the sense of a proton/non-proton pattern scheme was stressed. These measures increased the quantity of substructural properties covered by the intended fingerprint. In addition, alternative datasets of ABC transporter modulators⁵ and modes of action (particularly ABC transporter activators)^{6,8} have been considered to gain complementary knowledge about potentially active substructures. The resultant substructures were subsequently searched in the 1,167 compounds (loaded as.csv file) using the query search function of InstantJChem version 21.13.0 and, if present, listed in the substructure catalog. As a result, a catalog of 604 active substructures has been assembled.

Individual Pattern Analysis⁷. In a final step, the multitarget dataset of 1,167 compounds was statistically analyzed for the listed 604 substructures of the substructure catalog. Here, the resultant list of hit molecules per substructure derived from the query search function of InstantJChem version 21.13.0 was saved and compared to the original list, translating the entry differences into a binary code [1 = substructure present (active substructure); 0 = substructure not present (inactive substructure)]. A binary pattern distribution scheme resulted which constituted the final ABC_{BPMDS}. It shall be taken note that the number of the very same substructure within the same compound was irrelevant; the presence (numeric value = 1) of the substructure was not an expression of how often the respective substructure appeared within the compound.

Data Records

The ABC_{BPMDS} is freely available in an .xlsx format under the <http://www.zenodo.org>²⁸ URL as well as the <http://www.panabc.info> website and its use is free of charge. The dataset consists of (i) an individual database identifier for each compound; (ii) the original name of the compounds according to the original report(s); (iii) the IUPAC nomenclature of each compound generated by using ChemDraw Pro version 20.1.1.125; (iii) The SMILES code obtained either from the (a) supporting information of the respective report, (b) PubChem database (<https://pubchem.ncbi.nlm.nih.gov>), or (c) manual drawing using ChemDraw Pro version 20.1.1.125; (iv) the physicochemical properties (a) CLogP, (b) calculated molecular water solubility (CLogS), (c) MW, (d) MR, (e) TPSA, (f) H-bond donors, (g) H-bond acceptors, (h) rotatable bonds, and (j) number of heavy atoms; (v) the associated bioactivity values expressed as (a) IC₅₀ values [μM] against ABCB1, ABCC1, and ABCG2 presented in the standardized format of three significant digits as outlined above [10^{log(mean)}], and (b) pIC₅₀ values against ABCB1, ABCC1, and ABCG2; (vi) the binary code (active = 1; inactive = 0) for each of the 604 evaluated substructures of the substructure catalog including their (a) trivial name, (b) SMILES code, (c) number of defined hydrogens, (d) number of heavy atoms, (e) total hit count, and (f) individual substructure identifier. The substructures are sorted from most abundant (left) to most rare (right); and (vii) the PubMed (<https://pubmed.ncbi.nlm.nih.gov>) identifier (PMID) retrieved from NCBI (<https://www.ncbi.nlm.nih.gov>). In addition, a detailed curation protocol as well as an associated GraphPad Prism file can be found on <https://www.zenodo.org>⁵⁰ as well as the <http://www.panabc.info> website.

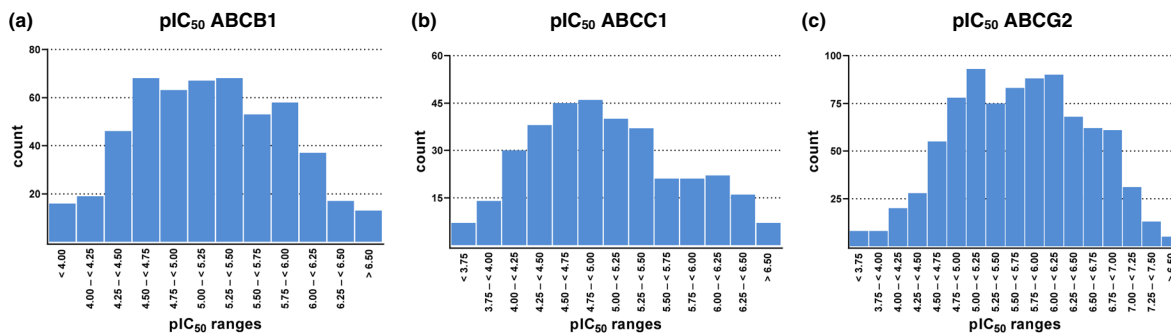


Fig. 2 Distribution of bioactivity values (pIC₅₀) of the 1,167 compounds of the ABC_BPMDS against ABCB1 (a), ABCC1 (b), and ABCG2 (c).

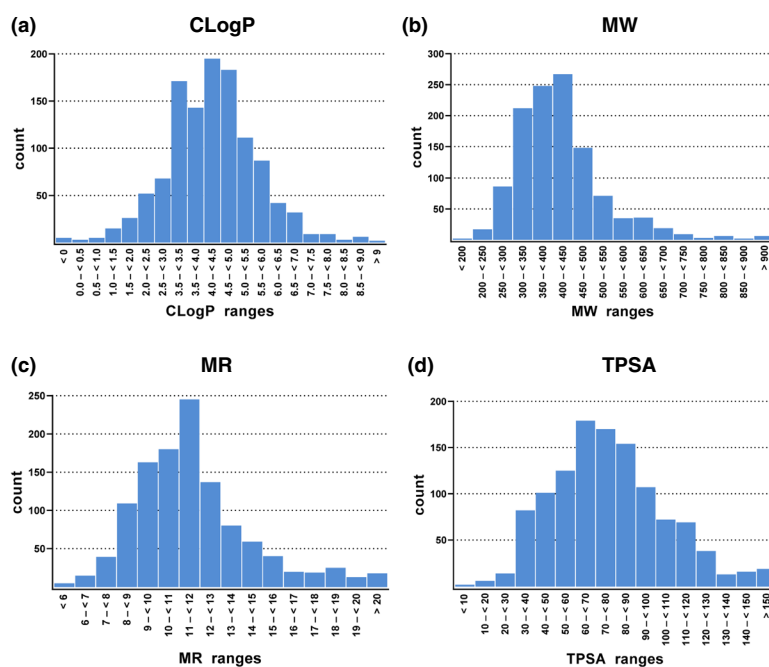


Fig. 3 Distribution of the important physicochemical¹¹⁵ properties CLogP (a), MW (b), MR (c), and TPSA (d) amongst the 1,167 compounds of the ABC_BPMDS as determined by MOE version 2019.01.

Technical Validation

Compounds. The 1,167 compounds were portrayed as canonical or isomeric SMILES codes as derived from the respective report or the PubChem database (<https://pubchem.ncbi.nlm.nih.gov>) and imported into the MarvinSketch editor implemented in InstantJChem version 21.13.0. If the loaded SMILES code appeared as the intended original molecular representation according to the respective report or the PubChem database (<https://pubchem.ncbi.nlm.nih.gov>) without any errors, it was considered as valid.

Bioactivity Space Validation. In total, 113 reports between 1994 and 2022 have been collected, resulting in a final number of 1,167 compounds that were evaluated against ABCB1, ABCC1, and ABCG2, including inactive compounds as well as selective, dual, and triple inhibitors. Amongst the 1,167 compounds are (i) 525 ABCB1 inhibitors, of which (a) 88 are selective ABCB1 inhibitors (no activity against ABCC1 and ABCG2; any given IC₅₀ value), (b) 67 are potent ABCB1 inhibitors (IC₅₀ values < 1 μM), and (c) 25 are selective and potent ABCB1 inhibitors; (ii) 344 ABCC1 inhibitors, of which (a) 61 are selective ABCC1 inhibitors (no activity against ABCB1 and ABCG2; any given IC₅₀ value), (b) 45 are potent ABCC1 inhibitors (IC₅₀ values < 1 μM), and (c) 11 are selective and potent ABCC1 inhibitors; (iii) 866 ABCG2 inhibitors, of which (a) 409 are selective ABCG2 inhibitors (no activity against ABCB1 and ABCC1; any given IC₅₀ value), (b) 330 are potent ABCG2 inhibitors (IC₅₀ values < 1 μM), and (c) 199 are selective and potent ABCG2 inhibitors.

On the other hand, 38, 212, and 58 dual ABCB1/ABCC1, ABCB1/ABCG2, and ABCC1/ABCG2 inhibitors are present, respectively, of which 7, 99, and 13 can be considered as potent dual ABCB1/ABCC1, ABCB1/ABCG2, and ABCC1/ABCG2 inhibitors, respectively (IC₅₀ < 10 μM). Finally, 187 triple ABCB1, ABCC1, and ABCG2 inhibitors can be defined, of which 54 can be considered as potent (IC₅₀ < 10 μM; so-called ‘Class 7’

inhibitor class	count	CLogP median	CLogP mean	MW median	MW mean	MR median	MR mean	TPSA median	TPSA mean
ABC_BPMDS	1,167	4.33	4.26	403.39	418.38	11.27	11.73	73.86	77.87
All ABCB1	525	4.40	4.78	432.43	458.67	12.07	12.90	73.63	79.56
All ABCC1	344	3.91	3.88	420.44	442.92	11.72	12.37	76.10	84.82
All ABCG2	866	4.34	4.25	396.37	415.32	11.13	11.64	74.73	79.01
Selective ABCB1	88	5.22	5.47	452.11	481.94	13.08	13.70	61.42	65.98
Selective ABCC1	61	3.37	3.41	374.49	377.22	11.07	10.70	69.77	75.29
Selective ABCG2	409	4.38	4.35	372.38	381.58	10.39	10.67	73.86	75.14
Dual ABCB1/ABCC1	38	5.03	4.80	475.56	471.03	13.19	13.20	70.05	78.29
Dual ABCC1/ABCG2	212	4.42	4.52	420.23	434.62	11.86	12.32	75.69	75.83
Dual ABCC1/ABCG2	58	3.62	3.68	376.91	398.33	10.52	11.23	76.26	80.98
Triple ABCB1/ABCC1/ABCG2	187	3.95	3.91	432.44	472.47	11.91	13.10	79.44	90.45

Table 4. Statistical survey of median and mean values of the important physicochemical properties CLogP, MW, MR, and TPSA amongst the entire ABC_BPMDS as well as important sub-classes as determined by MOE version 2019.01.

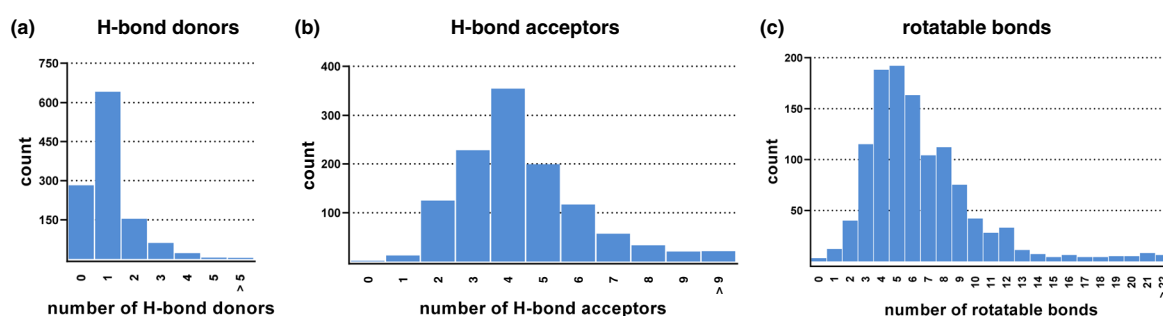


Fig. 4 Distribution of H-bond donors (a), H-bond acceptors (b), and rotatable bonds (c) amongst the 1,167 compounds of the ABC_BPMDS as determined by MOE version 2019.01.

compounds^{7,26,27}). Table 3 summarizes a survey of statistical parameters of the entire ABC_BPMDS as well as important sub-classes. Figure 2 depicts the distribution of the pIC_{50} values of ABCB1 (A), ABCC1 (B), and ABCG2 (C) inhibitors amongst the entire ABC_BPMDS, which followed in all three cases a Gaussian normal distribution.

Physicochemistry Space Validation. Physicochemical properties shape not only the pharmacological profile of ABC transporter inhibitors^{66–69}, but are also very often used as additional discriminators in virtual screening processes^{7,26,27,38}. To prove that the 1,167 compounds of the ABC_BPMDS have a balanced distribution of physicochemical attributes, the ABC_BPMDS was analyzed for the CLogP, MW, MR, and TPSA using MOE version 2019.01. Figure 3 demonstrates that these physicochemical properties are normally distributed within the ABC_BPMDS comparable to other reported datasets^{23,70}. Table 4 summarizes the median and mean values of CLogP, MW, MR, and TPSA of the entire ABC_BPMDS as well as important sub-classes. The median and mean values are well-aligned, which accounts for the equal distribution of values.

Molecular-Structure Space Validation. H-bonds and molecular flexibility are crucial aspects in terms of ligand-target interactions, especially for ABC transporters⁷¹. Hence, we analyzed the 1,167 compounds of the ABC_BPMDS for their number of H-bond donors, H-bond acceptors, and rotatable bonds. Figure 4 visualizes the found distributions amongst the entire ABC_BPMDS. Together with CLogP and MW, H-bond donors and acceptors play a major role in the drug-likeness as defined by Lipinski⁷², particularly influencing drug absorption, distribution, and permeation. Considering the ‘Lipinski rule of five’ (CLogP ≤ 5 ; MW ≤ 500 ; H-bond donors ≤ 5 ; H-bond acceptors ≤ 10), a large majority of compounds of the ABC_BPMDS fulfils these requirements. In particular, (i) 73.8% of compounds have CLogP values of ≤ 5 , (ii) 84.0% of compounds have a MW of ≤ 500 , (iii) 99.7% of compounds have ≤ 5 H-bond donors, and (iv) 98.6% of compounds have ≤ 10 H-bond acceptors. Table 5 summarizes the median and mean values of H-bond donors, H-bond acceptors, and rotatable bonds of the entire ABC_BPMDS as well as important sub-classes. Hence, the ABC_BPMDS contains suitable templates for future drug design and therapeutic development purposes, however, leaves also enough molecular-structural and physicochemical space for explorational analyses beyond the ‘Lipinski rule of five’ for the creation of inhomogeneous high-quality compound collections and compound libraries.

inhibitor class	count	H-bond donors median	H-bond donors mean	H-bond acceptors median	H-bond acceptors mean	rotatable bonds median	rotatable bonds mean
ABC_BPMDs	1,167	1	1.12	4	4.43	6	6.50
All ABCB1	525	1	1.07	4	4.95	7	7.72
All ABCC1	344	1	1.28	4	4.87	6	6.91
All ABCG2	866	1	1.15	4	4.42	5	6.51
Selective ABCB1	88	1	0.75	4	4.70	8	7.70
Selective ABCC1	61	1	1.46	4	4.03	6	5.57
Selective ABCG2	409	1	1.14	4	3.79	5	5.35
Dual ABCB1/ABCC1	38	1	0.895	4	4.32	6	6.74
Dual ABCC1/ABCG2	212	1	0.986	4	4.78	7	7.87
Dual ABCC1/ABCG2	58	1	1.14	4	4.40	4.5	5.66
Triple ABCB1/ABCC1/ABCG2	187	1	1.35	4	5.40	6	7.76

Table 5. Statistical survey of median and mean values of H-bond donors, H-bond acceptors, and rotatable bonds amongst the entire ABC_BPMDs as well as important sub-classes as determined by MOE version 2019.01.

Usage Notes

Status Quo. *Practical Use.* An easy-to-use sort function allows the user to discriminate the compounds regarding their bioactivities toward the targets, physicochemical properties, or molecular-structural features, but also in terms of the 604 different substructures. Hence, the user can retrieve the necessary binary pattern information for subsequent virtual screening and rational drug design approaches.

Special Considerations. The majority of the compounds was evaluated in proper full-blown concentration effect curves within the original report, providing either only one single IC₅₀ or two IC₅₀ values from different assays for biological validation, resulting mostly in minor standard deviations or standard errors. However, considering established reference compounds, many IC₅₀ values have been reported that are not fully covered by the deep literature search. Moreover, these drugs and drug-like compounds were tested in various assays, and thus, their IC₅₀ values vary in a greater span than of other compounds. In addition, data processing prior to the original publication varied from laboratory to laboratory [e.g., number of concentrations tested, manner of assay performance (non-standardized procedures), manner of data analysis (e.g., three- vs four-parameter logistic equation, relative vs absolute inhibition), data presentation (single-point screening graphic vs full-blown concentration effect curve, number of significant digits, in- or exclusion of standard deviation and/or standard error)] – contributing to a greater uncertainty of these particular data. Furthermore, the assays themselves that were considered for the ABC_BPMDs were various [e.g., influx vs efflux assay, fluorescence labeling vs radionuclide detection, manner of substrate (e.g., calcein AM vs mitoxantrone), selected cells vs transfected cells vs membrane vesicles] – contributing to a general variation in data that is hidden due to the fact that most compounds were only evaluated in one particular assessment system. These aspects should be considered when using the ABC_BPMDs, however, at the same time, it should be taken note that our previous work demonstrated the strength of substructural patterns based on the previous version of the ABC_BPMDs^{7,26,27}. A list of compounds affected by these variations in assessment systems can be found in the curation protocol under the <https://www.zenodo.org>⁵⁰ URL (<https://doi.org/10.5281/zenodo.6405752>) or on the <http://www.panabc.info> web site.

Future Perspective. *Extension – New Compounds.* The ABC_BPMDs provides the core application for extension to other, less- and under-studied ABC transporters. Particularly, the addressing of under-studied ABC transporters by multitarget agents poses a promising prospect for future drug discovery and development. Several compounds of the ABC_BPMDs have been demonstrated to address other ABC transporters as well^{5,25,26}, such as benzobromarone^{5,7,25–27}, cyclosporine A^{5,7,25–27}, dipyrindamole^{7,27,73–77}, erlotinib^{7,27,78,79}, imatinib^{5,7,25–27}, nilotinib^{7,27,78,80,81}, ritonavir^{7,27,82}, verapamil^{5,7,25–27}, and verlukast^{5,7,25–27,33}. These ‘truly multitarget pan-ABC transporter inhibitors’²⁵ are the primary focus for extension of the ABC_BPMDs, particularly with respect to their substructural elements that promote multitargeting. On the other hand, the addition of multitarget agents that are not part of the ABC_BPMDs will contribute valuable input to the polypharmacological space as charted by the future ABC_BPMDs_1.2.

Extension – New Substructures (‘ABC_BPMDs_1.2’). The substructural elements of the mentioned truly multitarget pan-ABC transporter inhibitors include 4-anilinoimidazole^{7,27}, benzyl⁷, cyano^{7,27}, 3,4-dimethoxyphenyl⁷, fluorine^{7,27}, furan^{7,26}, ethylene diamine⁷, ethylene hydroxy⁷, hydroxy⁷, isopropyl^{7,27}, methylene hydroxy⁷, phenethyl⁷, piperazine^{7,27}, pyrimidine^{7,26}, quinazoline^{7,27}, thiazole^{7,26}, and thioether⁷. These and other substructures will be re-evaluated with respect to true multitargeting, and thus, receive a differential value dependent on the purpose of the subsequent studies. Furthermore, the addition of multitarget agents that are not part of the ABC_BPMDs will contribute valuable input to the substructure catalog, extending the substructural output of

the future ABC_BPMDs_1.2. Specifically, this information beyond known multitarget fingerprints will enable the exploration and exploitation of under-studied ABC transporters as potential drug targets of the future.

Extension – New Modes and Targets. Particularly, the inclusion of, for example, different modes of modulation (e.g., activation), bioactivity measurements [e.g., *in vitro* (ATPase assays or MDR reversal assays), *in silico* binding mode analyses (e.g., molecular docking or molecular dynamics simulations), or structural information (e.g., x-ray, cryo-EM, homology-modelling, or AlphaFold⁸³)] will promote the discovery of drug candidates with distinctive mode of action. Furthermore, the logistics outlined in this work also provide a useful framework for similar data mining and descriptor approaches with respect to different pharmacological targets [e.g., under-studied human/bacterial ABC transporters, G-protein coupled receptors (GPCRs), ion channels (ICs), solute carriers (SLCs; PANSCLC, <http://www.panslcl.info>) or tyrosine kinases (TKs)].

Code availability

The ABC_BPMDs is available without any restrictions under the <http://www.zenodo.org>²⁸ URL (<https://doi.org/10.5281/zenodo.6384343>). In addition, a detailed curation protocol including a GraphPad Prism file are provided under the <https://www.zenodo.org>⁵⁰ URL (<https://doi.org/10.5281/zenodo.6405752>). All information is also available on the <http://www.panabc.info> website and the use is free of charge.

Received: 8 April 2022; Accepted: 28 June 2022;

Published online: 26 July 2022

References

- Wang, J. Q. *et al.* Multidrug resistance proteins (MRPs): Structure, function and the overcoming of cancer multidrug resistance. *Drug Resist Updat* **54**, 100743, <https://doi.org/10.1016/j.drug.2021.100743> (2021).
- Gil-Martins, E., Barbosa, D. J., Silva, V., Remiao, F. & Silva, R. Dysfunction of ABC transporters at the blood-brain barrier: Role in neurological disorders. *Pharmacol Ther* **213**, 107554, <https://doi.org/10.1016/j.pharmthera.2020.107554> (2020).
- Pasello, M., Giudice, A. M. & Scotlandi, K. The ABC subfamily A transporters: Multifaceted players with incipient potentialities in cancer. *Semin Cancer Biol* **60**, 57–71, <https://doi.org/10.1016/j.semcancer.2019.10.004> (2020).
- Sodani, K., Patel, A., Kathawala, R. J. & Chen, Z. S. Multidrug resistance associated proteins in multidrug resistance. *Chin J Cancer* **31**, 58–72, <https://doi.org/10.5732/cjc.011.10329> (2012).
- Pahnke, J. *et al.* Strategies to gain novel Alzheimer's disease diagnostics and therapeutics using modulators of ABCA transporters. *Free Neuropathol* **2**, <https://doi.org/10.17879/freeneuropathology-2021-3528> (2021).
- Wiese, M. & Stefan, S. M. The A-B-C of small-molecule ABC transport protein modulators: From inhibition to activation—a case study of multidrug resistance-associated protein 1 (ABCC1). *Med Res Rev* **39**, 2031–2081, <https://doi.org/10.1002/med.21573> (2019).
- Namasivayam, V. *et al.* Structural feature-driven pattern analysis for multitarget modulator landscapes. *Bioinformatics*, <https://doi.org/10.1093/bioinformatics/btab832> (2021).
- Stefan, S. M. & Wiese, M. Small-molecule inhibitors of multidrug resistance-associated protein 1 and related processes: A historic approach and recent advances. *Med Res Rev* **39**, 176–264, <https://doi.org/10.1002/med.21510> (2019).
- Hooper, A. J., Hegele, R. A. & Burnett, J. R. Tangier disease: update for 2020. *Curr Opin Lipidol* **31**, 80–84, <https://doi.org/10.1097/MOL.0000000000000669> (2020).
- Cremers, F. P. M., Lee, W., Collin, R. W. J. & Allikmets, R. Clinical spectrum, genetic complexity and therapeutic approaches for retinal disease caused by ABCA4 mutations. *Prog Retin Eye Res* **79**, 100861, <https://doi.org/10.1016/j.preteyeres.2020.100861> (2020).
- Elkhatib, A. M. & Omar, M. in *StatPearls* (2022).
- Bisaccia, F., Koshal, P., Abruzzese, V., Castiglione Morelli, M. A. & Ostuni, A. Structural and Functional Characterization of the ABCG6 Transporter in Hepatic Cells: Role on PXE, Cancer Therapy and Drug Resistance. *Int J Mol Sci* **22**, <https://doi.org/10.3390/ijms22062858> (2021).
- Turk, B. R., Theda, C., Fatemi, A. & Moser, A. B. X-linked adrenoleukodystrophy: Pathology, pathophysiology, diagnostic testing, newborn screening and therapies. *Int J Dev Neurosci* **80**, 52–72, <https://doi.org/10.1002/jdn.10003> (2020).
- Abdallah, I. M., Al-Shami, K. M., Yang, E. & Kaddoumi, A. Blood-Brain Barrier Disruption Increases Amyloid-Related Pathology in TgSwDI Mice. *Int J Mol Sci* **22**, <https://doi.org/10.3390/ijms22031231> (2021).
- Gomez-Zepeda, D., Taghi, M., Scherrmann, J. M., Deleves, X. & Menet, M. C. ABC Transporters at the Blood-Brain Interfaces, Their Study Models, and Drug Delivery Implications in Gliomas. *Pharmaceutics* **12**, <https://doi.org/10.3390/pharmaceutics12010020> (2019).
- Hernandez-Lozano, I. *et al.* PET imaging to assess the impact of P-glycoprotein on pulmonary drug delivery in rats. *J Control Release* **342**, 44–52, <https://doi.org/10.1016/j.jconrel.2021.12.031> (2022).
- Bruckmueller, H. & Cascorbi, I. ABCB1, ABCG2, ABCC1, ABCC2, and ABCC3 drug transporter polymorphisms and their impact on drug bioavailability: what is our current understanding? *Expert Opin Drug Metab Toxicol* **17**, 369–396, <https://doi.org/10.1080/17425255.2021.1876661> (2021).
- Girardin, F. Membrane transporter proteins: a challenge for CNS drug development. *Dialogues Clin Neurosci* **8**, 311–321 (2006).
- Cascorbi, I. Role of pharmacogenetics of ATP-binding cassette transporters in the pharmacokinetics of drugs. *Pharmacol Ther* **112**, 457–473, <https://doi.org/10.1016/j.pharmthera.2006.04.009> (2006).
- Kim, S. *et al.* PubChem Substance and Compound databases. *Nucleic Acids Res* **44**, D1202–D1213, <https://doi.org/10.1093/nar/gkv951> (2016).
- Rogers, D. & Hahn, M. Extended-connectivity fingerprints. *J Chem Inf Model* **50**, 742–754, <https://doi.org/10.1021/ci100050t> (2010).
- Bender, A., Mussa, H. Y., Glen, R. C. & Reiling, S. Molecular similarity searching using atom environments, information-based feature selection, and a naive Bayesian classifier. *J Chem Inf Comput Sci* **44**, 170–178, <https://doi.org/10.1021/ci034207y> (2004).
- Meng, F., Xi, Y., Huang, J. & Ayers, P. W. A curated diverse molecular database of blood-brain barrier permeability with chemical descriptors. *Sci Data* **8**, 289, <https://doi.org/10.1038/s41597-021-01069-5> (2021).
- Stefan, S. M. Multi-target ABC transporter modulators: what next and where to go. *Future Med Chem* **11**, 2353–2358, <https://doi.org/10.4155/fmc-2019-0185> (2019).
- Namasivayam, V., Stefan, K., Pahnke, J. & Stefan, S. M. Binding mode analysis of ABCA7 for the prediction of novel Alzheimer's disease therapeutics. *Comput Struct Biotechnol J* **19**, 6490–6504, <https://doi.org/10.1016/j.csbj.2021.11.035> (2021).

26. Namasivayam, V., Silbermann, K., Pahnke, J., Wiese, M. & Stefan, S. M. Scaffold fragmentation and substructure hopping reveal potential, robustness, and limits of computer-aided pattern analysis (C@PA). *Comput Struct Biotechnol J* **19**, 3269–3283, <https://doi.org/10.1016/j.csbj.2021.05.018> (2021).
27. Namasivayam, V., Silbermann, K., Wiese, M., Pahnke, J. & Stefan, S. M. C@PA: Computer-Aided Pattern Analysis to Predict Multitarget ABC Transporter Inhibitors. *J Med Chem* **64**, 3350–3366, <https://doi.org/10.1021/acs.jmedchem.0c02199> (2021).
28. Stefan, S. M., Jansson, P. J., Pahnke, J. & Namasivayam, V. A curated binary pattern multitarget dataset of focused ABC transporter inhibitors. *zenodo* <https://doi.org/10.5281/zenodo.6384343> (2022).
29. Benson, D., Boguski, M., Lipman, D. & Ostell, J. The National Center for Biotechnology Information. *Genomics* **6**, 389–391, [https://doi.org/10.1016/0888-7543\(90\)90583-g](https://doi.org/10.1016/0888-7543(90)90583-g) (1990).
30. Weidner, L. D. *et al.* The Inhibitor Ko143 Is Not Specific for ABCG2. *J Pharmacol Exp Ther* **354**, 384–393, <https://doi.org/10.1124/jpet.115.225482> (2015).
31. Peterson, B. G., Tan, K. W., Osa-Andrews, B. & Iram, S. H. High-content screening of clinically tested anticancer drugs identifies novel inhibitors of human MRP1 (ABCC1). *Pharmacol Res* **119**, 313–326, <https://doi.org/10.1016/j.phrs.2017.02.024> (2017).
32. Csandl, M. A., Conseil, G. & Cole, S. P. Cysteinyln Leukotriene Receptor 1/2 Antagonists Nonselectively Modulate Organic Anion Transport by Multidrug Resistance Proteins (MRP1-4). *Drug Metab Dispos* **44**, 857–866, <https://doi.org/10.1124/dmd.116.069468> (2016).
33. Matsson, P., Pedersen, J. M., Norinder, U., Bergstrom, C. A. & Artursson, P. Identification of novel specific and general inhibitors of the three major human ATP-binding cassette transporters P-gp, BCRP and MRP2 among registered drugs. *Pharm Res* **26**, 1816–1831, <https://doi.org/10.1007/s11095-009-9896-0> (2009).
34. Wu, C. P., Klokouzas, A., Hladky, S. B., Ambudkar, S. V. & Barrand, M. A. Interactions of mefloquine with ABC proteins, MRP1 (ABCC1) and MRP4 (ABCC4) that are present in human red cell membranes. *Biochem Pharmacol* **70**, 500–510, <https://doi.org/10.1016/j.bcp.2005.05.022> (2005).
35. Mrowczynska, L., Bobrowska-Hagerstrand, M., Wrobel, A., Soderstrom, T. & Hagerstrand, H. Inhibition of MRP1-mediated efflux in human erythrocytes by mono-anionic bile salts. *Anticancer Res* **25**, 3173–3178 (2005).
36. Leier, I., Jedlitschky, G., Buchholz, U. & Keppler, D. Characterization of the ATP-dependent leukotriene C4 export carrier in mastocytoma cells. *Eur J Biochem* **220**, 599–606, <https://doi.org/10.1111/j.1432-1033.1994.tb18661.x> (1994).
37. Shang, S. & Tan, D. S. Advancing chemistry and biology through diversity-oriented synthesis of natural product-like libraries. *Curr Opin Chem Biol* **9**, 248–258, <https://doi.org/10.1016/j.cbpa.2005.03.006> (2005).
38. Silbermann, K., Stefan, S. M., Elshawadfy, R., Namasivayam, V. & Wiese, M. Identification of Thienopyrimidine Scaffold as an Inhibitor of the ABC Transport Protein ABCC1 (MRP1) and Related Transporters Using a Combined Virtual Screening Approach. *J Med Chem* **62**, 4383–4400, <https://doi.org/10.1021/acs.jmedchem.8b01821> (2019).
39. Riganti, C. *et al.* Design, Biological Evaluation, and Molecular Modeling of Tetrahydroisoquinoline Derivatives: Discovery of A Potent P-Glycoprotein Ligand Overcoming Multidrug Resistance in Cancer Stem Cells. *J Med Chem* **62**, 974–986, <https://doi.org/10.1021/acs.jmedchem.8b01655> (2019).
40. Vagiannis, D. *et al.* Alisertib shows negligible potential for perpetrating pharmacokinetic drug-drug interactions on ABCB1, ABCG2 and cytochromes P450, but acts as dual-activity resistance modulator through the inhibition of ABCC1 transporter. *Toxicol Appl Pharmacol* **434**, 115823, <https://doi.org/10.1016/j.taap.2021.115823> (2022).
41. Dakhlou, I. *et al.* Synthesis and biological assessment of new pyrimidopyrimidines as inhibitors of breast cancer resistance protein (ABCG2). *Bioorg Chem* **116**, 105326, <https://doi.org/10.1016/j.bioorg.2021.105326> (2021).
42. To, K. K. W. *et al.* Reversal of multidrug resistance by *Marsdenia tenacissima* and its main active ingredients polyoxypregnanes. *J Ethnopharmacol* **203**, 110–119, <https://doi.org/10.1016/j.jep.2017.03.051> (2017).
43. Muller, H. *et al.* New functional assay of P-glycoprotein activity using Hoechst 33342. *Bioorg Med Chem* **15**, 7470–7479, <https://doi.org/10.1016/j.bmc.2007.07.024> (2007).
44. Silbermann, K., Li, J., Namasivayam, V., Stefan, S. M. & Wiese, M. Rational drug design of 6-substituted 4-anilino-2-phenylpyrimidines for exploration of novel ABCG2 binding site. *Eur J Med Chem* **212**, 113045, <https://doi.org/10.1016/j.ejmech.2020.113045> (2021).
45. Silbermann, K. *et al.* Superior Pyrimidine Derivatives as Selective ABCG2 Inhibitors and Broad-Spectrum ABCB1, ABCC1, and ABCG2 Antagonists. *J Med Chem* **63**, 10412–10432, <https://doi.org/10.1021/acs.jmedchem.0c00961> (2020).
46. Krapf, M. K. & Wiese, M. Synthesis and Biological Evaluation of 4-Anilino-quinazolines and -quinolines as Inhibitors of Breast Cancer Resistance Protein (ABCG2). *J Med Chem* **59**, 5449–5461, <https://doi.org/10.1021/acs.jmedchem.6b00330> (2016).
47. Bi, X. *et al.* Piperine enhances the bioavailability of silybin via inhibition of efflux transporters BCRP and MRP2. *Phytomedicine* **54**, 98–108, <https://doi.org/10.1016/j.phymed.2018.09.217> (2019).
48. Mi, Y. J. *et al.* Apatinib (YN968D1) reverses multidrug resistance by inhibiting the efflux function of multiple ATP-binding cassette transporters. *Cancer Res* **70**, 7981–7991, <https://doi.org/10.1158/0008-5472.CAN-10-0111> (2010).
49. Hu, J. *et al.* Effect of ceritinib (LDK378) on enhancement of chemotherapeutic agents in ABCB1 and ABCG2 overexpressing cells in vitro and in vivo. *Oncotarget* **6**, 44643–44659, <https://doi.org/10.18632/oncotarget.5989> (2015).
50. Stefan, S. M., Jansson, P. J., Pahnke, J. & Namasivayam, V. Supplementary Information - A curated binary pattern multitarget dataset of focused ABC transporter inhibitors. *zenodo* <https://doi.org/10.5281/zenodo.6405752> (2022).
51. Pick, A. *et al.* Structure-activity relationships of flavonoids as inhibitors of breast cancer resistance protein (BCRP). *Bioorg Med Chem* **19**, 2090–2102, <https://doi.org/10.1016/j.bmc.2010.12.043> (2011).
52. Juvala, K., Stefan, K. & Wiese, M. Synthesis and biological evaluation of flavones and benzoflavones as inhibitors of BCRP/ABCG2. *Eur J Med Chem* **67**, 115–126, <https://doi.org/10.1016/j.ejmech.2013.06.035> (2013).
53. Gu, X. *et al.* Discovery of alkoxy biphenyl derivatives bearing dibenzo[c,e]azepine scaffold as potential dual inhibitors of P-glycoprotein and breast cancer resistance protein. *Bioorg Med Chem Lett* **24**, 3419–3421, <https://doi.org/10.1016/j.bmcl.2014.05.081> (2014).
54. Paterna, A. *et al.* Monoterpene indole alkaloid azine derivatives as MDR reversal agents. *Bioorg Med Chem* **26**, 421–434, <https://doi.org/10.1016/j.bmc.2017.11.052> (2018).
55. Chearwae, W. *et al.* Curcuminoids purified from turmeric powder modulate the function of human multidrug resistance protein 1 (ABCC1). *Cancer Chemother Pharmacol* **57**, 376–388, <https://doi.org/10.1007/s00280-005-0052-1> (2006).
56. Ozvegy-Laczka, C. *et al.* High-affinity interaction of tyrosine kinase inhibitors with the ABCG2 multidrug transporter. *Mol Pharmacol* **65**, 1485–1495, <https://doi.org/10.1124/mol.65.6.1485> (2004).
57. Antoni, F. *et al.* Tariquidar-related triazoles as potent, selective and stable inhibitors of ABCG2 (BCRP). *Eur J Med Chem* **191**, 112133, <https://doi.org/10.1016/j.ejmech.2020.112133> (2020).
58. Krapf, M. K., Gallus, J. & Wiese, M. Synthesis and biological investigation of 2,4-substituted quinazolines as highly potent inhibitors of breast cancer resistance protein (ABCG2). *Eur J Med Chem* **139**, 587–611, <https://doi.org/10.1016/j.ejmech.2017.08.020> (2017).
59. Pick, A. & Wiese, M. Tyrosine kinase inhibitors influence ABCG2 expression in EGFR-positive MDCK BCRP cells via the PI3K/Akt signaling pathway. *ChemMedChem* **7**, 650–662, <https://doi.org/10.1002/cmdc.201100543> (2012).
60. Obrique-Balboa, J. E., Sun, Q., Bernhardt, G., Konig, B. & Buschauer, A. Flavonoid derivatives as selective ABCC1 modulators: Synthesis and functional characterization. *Eur J Med Chem* **109**, 124–133, <https://doi.org/10.1016/j.ejmech.2015.12.010> (2016).

61. Juvale, K., Gallus, J. & Wiese, M. Investigation of quinazolines as inhibitors of breast cancer resistance protein (ABCG2). *Bioorg Med Chem* **21**, 7858–7873, <https://doi.org/10.1016/j.bmc.2013.10.007> (2013).
62. Juvale, K. & Wiese, M. 4-Substituted-2-phenylquinazolines as inhibitors of BCRP. *Bioorg Med Chem Lett* **22**, 6766–6769, <https://doi.org/10.1016/j.bmcl.2012.08.024> (2012).
63. Schafer, A., Kohler, S. C., Lohe, M., Wiese, M. & Hiersemann, M. Synthesis of Homoverrucosanoid-Derived Esters and Evaluation as MDR Modulators. *J Org Chem* **82**, 10504–10522, <https://doi.org/10.1021/acs.joc.7b02012> (2017).
64. Durant, J. L., Leland, B. A., Henry, D. R. & Nourse, J. G. Reoptimization of MDL keys for use in drug discovery. *J Chem Inf Comput Sci* **42**, 1273–1280, <https://doi.org/10.1021/ci010132r> (2002).
65. Jordan, A. M. & Roughley, S. D. Drug discovery chemistry: a primer for the non-specialist. *Drug Discov Today* **14**, 731–744, <https://doi.org/10.1016/j.drudis.2009.04.005> (2009).
66. Schmitt, S. M., Stefan, K. & Wiese, M. Pyrrolopyrimidine Derivatives as Novel Inhibitors of Multidrug Resistance-Associated Protein 1 (MRP1, ABCC1). *J Med Chem* **59**, 3018–3033, <https://doi.org/10.1021/acs.jmedchem.5b01644> (2016).
67. Marighetti, F., Steggemann, K., Karbaum, M. & Wiese, M. Scaffold identification of a new class of potent and selective BCRP inhibitors. *ChemMedChem* **10**, 742–751, <https://doi.org/10.1002/cmdc.201402498> (2015).
68. Marighetti, F., Steggemann, K., Hanl, M. & Wiese, M. Synthesis and quantitative structure-activity relationships of selective BCRP inhibitors. *ChemMedChem* **8**, 125–135, <https://doi.org/10.1002/cmdc.201200377> (2013).
69. Stefan, S. M. *Purines and 9-deazapurines as Modulators of Multidrug Resistance-associated Protein 1 (MRP1/ABCC1)-mediated Transport* 14.11.2017 edn, 1 (2017).
70. Stepanov, D., Canipa, S. & Wolber, G. HuskinDB, a database for skin permeation of xenobiotics. *Sci Data* **7**, 426, <https://doi.org/10.1038/s41597-020-00764-z> (2020).
71. Pajeva, I. K. & Wiese, M. Pharmacophore model of drugs involved in P-glycoprotein multidrug resistance: explanation of structural variety (hypothesis). *J Med Chem* **45**, 5671–5686, <https://doi.org/10.1021/jm020941h> (2002).
72. Lipinski, C. A., Lombardo, F., Dominy, B. W. & Feeney, P. J. Experimental and computational approaches to estimate solubility and permeability in drug discovery and development settings. *Adv Drug Deliv Rev* **46**, 3–26, [https://doi.org/10.1016/s0169-409x\(00\)00129-0](https://doi.org/10.1016/s0169-409x(00)00129-0) (2001).
73. Bieczynski, F., Burkhardt-Medicke, K., Luquet, C. M., Scholz, S. & Luckenbach, T. Chemical effects on dye efflux activity in live zebrafish embryos and on zebrafish Abcb4 ATPase activity. *FEBS Lett* **595**, 828–843, <https://doi.org/10.1002/1873-3468.14015> (2021).
74. Schadt, S. *et al.* Minimizing DILI risk in drug discovery - A screening tool for drug candidates. *Toxicol In Vitro* **30**, 429–437, <https://doi.org/10.1016/j.tiv.2015.09.019> (2015).
75. Sager, G. *et al.* Novel cGMP efflux inhibitors identified by virtual ligand screening (VLS) and confirmed by experimental studies. *J Med Chem* **55**, 3049–3057, <https://doi.org/10.1021/jm2014666> (2012).
76. Wu, C. P., Calcagno, A. M., Hladky, S. B., Ambudkar, S. V. & Barrand, M. A. Modulatory effects of plant phenols on human multidrug-resistance proteins 1, 4 and 5 (ABCC1, 4 and 5). *FEBS J* **272**, 4725–4740, <https://doi.org/10.1111/j.1742-4658.2005.04888.x> (2005).
77. Smeets, P. H., van Aubel, R. A., Wouterse, A. C., van den Heuvel, J. J. & Russel, F. G. Contribution of multidrug resistance protein 2 (MRP2/ABCC2) to the renal excretion of p-aminohippurate (PAH) and identification of MRP4 (ABCC4) as a novel PAH transporter. *J Am Soc Nephrol* **15**, 2828–2835, <https://doi.org/10.1097/01.ASN.0000143473.64430.AC> (2004).
78. Beretta, G. L., Cassinelli, G., Pennati, M., Zuco, V. & Gatti, L. Overcoming ABC transporter-mediated multidrug resistance: The dual role of tyrosine kinase inhibitors as multitargeting agents. *Eur J Med Chem* **142**, 271–289, <https://doi.org/10.1016/j.ejmech.2017.07.062> (2017).
79. Cheung, L. *et al.* Identification of new MRP4 inhibitors from a library of FDA approved drugs using a high-throughput bioluminescence screen. *Biochem Pharmacol* **93**, 380–388, <https://doi.org/10.1016/j.bcp.2014.11.006> (2015).
80. Eadie, L. N., Dang, P., Goyne, J. M., Hughes, T. P. & White, D. L. ABCC6 plays a significant role in the transport of nilotinib and dasatinib, and contributes to TKI resistance in vitro, in both cell lines and primary patient mononuclear cells. *PLoS One* **13**, e0192180, <https://doi.org/10.1371/journal.pone.0192180> (2018).
81. Hupfeld, T. *et al.* Tyrosinekinase inhibition facilitates cooperation of transcription factor SALL4 and ABC transporter A3 towards intrinsic CML cell drug resistance. *Br J Haematol* **161**, 204–213, <https://doi.org/10.1111/bjh.12246> (2013).
82. Ambrus, C., Bakos, E., Sarkadi, B., Ozvegy-Laczka, C. & Telbisz, A. Interactions of anti-COVID-19 drug candidates with hepatic transporters may cause liver toxicity and affect pharmacokinetics. *Sci Rep* **11**, 17810, <https://doi.org/10.1038/s41598-021-97160-3> (2021).
83. Jumper, J. *et al.* Highly accurate protein structure prediction with AlphaFold. *Nature* **596**, 583–589, <https://doi.org/10.1038/s41586-021-03819-2> (2021).
84. Chearwae, W., Anuchapreeda, S., Nandigama, K., Ambudkar, S. V. & Limtrakul, P. Biochemical mechanism of modulation of human P-glycoprotein (ABCB1) by curcumin I, II, and III purified from Turmeric powder. *Biochem Pharmacol* **68**, 2043–2052, <https://doi.org/10.1016/j.bcp.2004.07.009> (2004).
85. Dohse, M. *et al.* Comparison of ATP-binding cassette transporter interactions with the tyrosine kinase inhibitors imatinib, nilotinib, and dasatinib. *Drug Metab Dispos* **38**, 1371–1380, <https://doi.org/10.1124/dmd.109.031302> (2010).
86. Colabufo, N. A. *et al.* Multi-drug-resistance-reverting agents: 2-aryloxazole and 2-arylthiazole derivatives as potent BCRP or MRP1 inhibitors. *ChemMedChem* **4**, 188–195, <https://doi.org/10.1002/cmdc.200800329> (2009).
87. Jekerle, V. *et al.* In vitro and in vivo evaluation of WK-X-34, a novel inhibitor of P-glycoprotein and BCRP, using radio imaging techniques. *Int J Cancer* **119**, 414–422, <https://doi.org/10.1002/ijc.21827> (2006).
88. Mathias, T. J. *et al.* The FLT3 and PDGFR inhibitor crenolanib is a substrate of the multidrug resistance protein ABCB1 but does not inhibit transport function at pharmacologically relevant concentrations. *Invest New Drugs* **33**, 300–309, <https://doi.org/10.1007/s10637-015-0205-y> (2015).
89. Telbisz, A. *et al.* Interactions of Potential Anti-COVID-19 Compounds with Multispecific ABC and OATP Drug Transporters. *Pharmaceutics* **13**, <https://doi.org/10.3390/pharmaceutics13010081> (2021).
90. Zhang, Y., Latterra, J. & Pomper, M. G. Hedgehog pathway inhibitor HhAntag691 is a potent inhibitor of ABCG2/BCRP and ABCB1/Pgp. *Neoplasia* **11**, 96–101, <https://doi.org/10.1593/neo.81264> (2009).
91. Vagiannis, D., Yu, Z., Novotna, E., Morell, A. & Hofman, J. Entrectinib reverses cytoskeletal resistance through the inhibition of ABCB1 efflux transporter, but not the CYP3A4 drug-metabolizing enzyme. *Biochem Pharmacol* **178**, 114061, <https://doi.org/10.1016/j.bcp.2020.114061> (2020).
92. Tan, K. W., Sampson, A., Osa-Andrews, B. & Iram, S. H. Calcitriol and Calcipotriol Modulate Transport Activity of ABC Transporters and Exhibit Selective Cytotoxicity in MRP1-overexpressing Cells. *Drug Metab Dispos* **46**, 1856–1866, <https://doi.org/10.1124/dmd.118.081612> (2018).
93. Lempers, V. J. *et al.* Inhibitory Potential of Antifungal Drugs on ATP-Binding Cassette Transporters P-Glycoprotein, MRP1 to MRP5, BCRP, and BSEP. *Antimicrob Agents Chemother* **60**, 3372–3379, <https://doi.org/10.1128/AAC.02931-15> (2016).
94. Holland, M. L., Allen, J. D. & Arnold, J. C. Interaction of plant cannabinoids with the multidrug transporter ABCC1 (MRP1). *Eur J Pharmacol* **591**, 128–131, <https://doi.org/10.1016/j.ejphar.2008.06.079> (2008).
95. Teodori, E. *et al.* Design, synthesis and biological evaluation of stereo- and regioisomers of amino aryl esters as multidrug resistance (MDR) reversers. *Eur J Med Chem* **182**, 111655, <https://doi.org/10.1016/j.ejmech.2019.111655> (2019).

96. Scoparo, C. T. *et al.* Dual properties of hispidulin: antiproliferative effects on HepG2 cancer cells and selective inhibition of ABCG2 transport activity. *Mol Cell Biochem* **409**, 123–133, <https://doi.org/10.1007/s11010-015-2518-8> (2015).
97. Pawarode, A. *et al.* Differential effects of the immunosuppressive agents cyclosporin A, tacrolimus and sirolimus on drug transport by multidrug resistance proteins. *Cancer Chemother Pharmacol* **60**, 179–188, <https://doi.org/10.1007/s00280-006-0357-8> (2007).
98. Huang, X. C., Sun, Y. L., Salim, A. A., Chen, Z. S. & Capon, R. J. Parguerenes: Marine red alga bromoditerpenes as inhibitors of P-glycoprotein (ABCB1) in multidrug resistant human cancer cells. *Biochem Pharmacol* **85**, 1257–1268, <https://doi.org/10.1016/j.bcp.2013.02.005> (2013).
99. Kita, D. H. *et al.* Mechanistic basis of breast cancer resistance protein inhibition by new indeno[1,2-b]indoles. *Sci Rep* **11**, 1788, <https://doi.org/10.1038/s41598-020-79892-w> (2021).
100. Munoz-Martinez, F. *et al.* Celastraceae sesquiterpenes as a new class of modulators that bind specifically to human P-glycoprotein and reverse cellular multidrug resistance. *Cancer Res* **64**, 7130–7138, <https://doi.org/10.1158/0008-5472.CAN-04-1005> (2004).
101. Sun, S. *et al.* The two enantiomers of tetrahydropalmitate are inhibitors of P-gp, but not inhibitors of MRP1 or BCRP. *Xenobiotica* **42**, 1197–1205, <https://doi.org/10.3109/00498254.2012.702247> (2012).
102. Sen, R. *et al.* The novel BCR-ABL and FLT3 inhibitor ponatinib is a potent inhibitor of the MDR-associated ATP-binding cassette transporter ABCG2. *Mol Cancer Ther* **11**, 2033–2044, <https://doi.org/10.1158/1535-7163.MCT-12-0302> (2012).
103. Li, S. *et al.* Piperine, a piperidine alkaloid from Piper nigrum re-sensitizes P-gp, MRP1 and BCRP dependent multidrug resistant cancer cells. *Phytomedicine* **19**, 83–87, <https://doi.org/10.1016/j.phymed.2011.06.031> (2011).
104. Zhu, H. J. *et al.* Characterization of P-glycoprotein inhibition by major cannabinoids from marijuana. *J Pharmacol Exp Ther* **317**, 850–857, <https://doi.org/10.1124/jpet.105.098541> (2006).
105. Ivnitski-Steele, I. *et al.* High-throughput flow cytometry to detect selective inhibitors of ABCB1, ABCC1, and ABCG2 transporters. *Assay Drug Dev Technol* **6**, 263–276, <https://doi.org/10.1089/adt.2007.107> (2008).
106. Teng, Y. N. *et al.* beta-carotene reverses multidrug resistant cancer cells by selectively modulating human P-glycoprotein function. *Phytomedicine* **23**, 316–323, <https://doi.org/10.1016/j.phymed.2016.01.008> (2016).
107. Kannan, P. *et al.* The "specific" P-glycoprotein inhibitor Tariquidar is also a substrate and an inhibitor for breast cancer resistance protein (BCRP/ABCG2). *ACS Chem Neurosci* **2**, 82–89, <https://doi.org/10.1021/cn100078a> (2011).
108. Sachs, J. *et al.* Novel 3,4-Dihydroisocoumarins Inhibit Human P-gp and BCRP in Multidrug Resistant Tumors and Demonstrate Substrate Inhibition of Yeast Pdr5. *Front Pharmacol* **10**, 400, <https://doi.org/10.3389/fphar.2019.00400> (2019).
109. Gu, X. *et al.* Synthesis and biological evaluation of novel bifendate derivatives bearing 6,7-dihydro-dibenzo[c,e]azepine scaffold as potent P-glycoprotein inhibitors. *Eur J Med Chem* **51**, 137–144, <https://doi.org/10.1016/j.ejmech.2012.02.034> (2012).
110. Ma, S. L. *et al.* Lapatinib antagonizes multidrug resistance-associated protein 1-mediated multidrug resistance by inhibiting its transport function. *Mol Med* **20**, 390–399, <https://doi.org/10.2119/molmed.2014.00059> (2014).
111. Wu, C. P. *et al.* Overexpression of ATP-binding cassette transporter ABCG2 as a potential mechanism of acquired resistance to vemurafenib in BRAF(V600E) mutant cancer cells. *Biochem Pharmacol* **85**, 325–334, <https://doi.org/10.1016/j.bcp.2012.11.003> (2013).
112. Rijpmma, S. R. *et al.* Atovaquone and quinine anti-malarials inhibit ATP binding cassette transporter activity. *Malar J* **13**, 359, <https://doi.org/10.1186/1475-2875-13-359> (2014).
113. Holland, M. L., Lau, D. T., Allen, J. D. & Arnold, J. C. The multidrug transporter ABCG2 (BCRP) is inhibited by plant-derived cannabinoids. *Br J Pharmacol* **152**, 815–824, <https://doi.org/10.1038/sj.bjp.0707467> (2007).
114. Krauze, A. *et al.* Thieno[2,3-b]pyridines—a new class of multidrug resistance (MDR) modulators. *Bioorg Med Chem* **22**, 5860–5870, <https://doi.org/10.1016/j.bmc.2014.09.023> (2014).
115. Namasivayam, V. *et al.* Physicochemistry shapes bioactivity landscape of pan-ABC transporter modulators: anchor point for innovative Alzheimer's disease therapeutics. *Int J Biol Macromol* <https://doi.org/10.1016/j.ijbiomac.2022.07.062> (2022).

Acknowledgements

S.M.S. is supported by the Walter Benjamin and Research Grant Programmes of the German Research Foundation [DFG, Deutsche Forschungsgemeinschaft, Germany; #446812474, #504079349 (PANABC)]. P.J.J. appreciates the Cancer Institute of New South Wales Career Development Fellowship (#CDF171147) support. J.P. received funding from the DFG (Germany; #263024513), Nasjonalforeningen (Norway; #16154), HelseSØ (Norway, #2019054, #2019055, #2022046), Barnekreftforeningen (Norway; #19008), EEA and Norway grants Kappa programme [Iceland, Liechtenstein, Norway, Czech Republic; #TO100078 (TAČR TARIMAD)], Norges forskningsråd [Norway; #295910 (NAPI), #327571 (PETABC)], and the European Commission (European Union; #643417). PETABC is an EU Joint Programme - Neurodegenerative Disease Research (JPND) project. PETABC is supported through the following funding organizations under the aegis of JPND – www.jpnd.eu: NFR #327571 – Norway; FFG #882717 – Austria; BMBF #01ED2106 – Germany; MSMT #8F21002 – Czech Republic; VAA #ES RTD/2020/26 – Latvia; ANR #20-JPW2-0002-04 – France, SRC #2020-02905 – Sweden. The projects receive funding from the European Union's Horizon 2020 research and innovation programme under grant agreement #643417 (JPco-fuND). V.N. is supported by the Research Grant Programme of the DFG [#504079349 (PANABC)]. The authors like to thank ChemAxon for providing academic research license for InstantJChem.

Author contributions

S.M.S. Conceptualization, Methodology, Validation, Formal Analysis, Data Curation, Writing – Original Draft, Writing – Review & Editing, Visualization, Project Administration, Funding Acquisition. P.J.J. Resources, Writing – Review & Editing, Visualization, Funding Acquisition. J.P. Resources, Writing – Review & Editing, Funding Acquisition. V.N. Conceptualization, Methodology, Software, Validation, Formal Analysis, Data Curation, Writing – Review & Editing, Visualization, Project Administration.

Funding

Open Access funding enabled and organized by Projekt DEAL.

Competing interests

The authors declare no competing interests.

Additional information

Correspondence and requests for materials should be addressed to V.N.

Reprints and permissions information is available at www.nature.com/reprints.

Publisher's note Springer Nature remains neutral with regard to jurisdictional claims in published maps and institutional affiliations.



Open Access This article is licensed under a Creative Commons Attribution 4.0 International License, which permits use, sharing, adaptation, distribution and reproduction in any medium or format, as long as you give appropriate credit to the original author(s) and the source, provide a link to the Creative Commons license, and indicate if changes were made. The images or other third party material in this article are included in the article's Creative Commons license, unless indicated otherwise in a credit line to the material. If material is not included in the article's Creative Commons license and your intended use is not permitted by statutory regulation or exceeds the permitted use, you will need to obtain permission directly from the copyright holder. To view a copy of this license, visit <http://creativecommons.org/licenses/by/4.0/>.

© The Author(s) 2022